Acta Crystallographica Section D
Biological Crystallography
ISSN 1399-0047

Conformational transitions in the γ subunit of the archaeal translation initiation factor 2

Oleg Nikonov,* Elena Stolboushkina, Valentina Arkhipova, Olesya Kravchenko, Stanislav Nikonov and Maria Garber

Institute of Protein Research, Russian Academy of Sciences, Pushchino 142290, Moscow Region, Russian Federation

Correspondence e-mail: alik@vega.protres.ru

Received 31 August 2013
Accepted 26 November 2013

PDB references: aIF2γ–GDP, 4m0l; nucleotide-free aIF2γ, 4m2l; aIF2γ–GDP–formate, 4m4s; aIF2γ–GDPCP, 4m53

In eukaryotes and archaea, the heterotrimeric translation initiation factor 2 (e/aIF2) is pivotal for the delivery of methionylated initiator tRNA (Met-tRNA$_i$) to the ribosome. It acts as a molecular switch that cycles between inactive (GDP-bound) and active (GTP-bound) states. Recent studies show that eIF2 can also exist in a long-lived eIF2γ–GDP–P$_i$ (inorganic phosphate) active state. Here, four high-resolution crystal structures of aIF2γ from *Sulfolobus solfataricus* are reported: aIF2γ–GDPCP (a nonhydrolyzable GTP analogue), aIF2γ–GDP–formate (in which a formate ion possibly mimics P$_i$), aIF2γ–GDP and nucleotide-free aIF2γ. The structures describe the different states of aIF2γ and demonstrate the conformational transitions that take place in the aIF2γ 'life cycle'.

1. Introduction

Heterotrimeric ($\alpha\beta\gamma$) translation initiation factor 2 (e/aIF2) in its GTP-bound state interacts specifically with methionylated initiator tRNA (Met-tRNA$_i$) and contributes to its adjustment in the ribosomal P site. Both the eukaryotic translation initiation factor (eIF2) and the archaeal translation initiation factor (aIF2) have three subunits: α, β and γ. The γ subunit belongs to the superfamily of GTP-binding proteins, and in the case of aIF2γ it is most closely related to the translation elongation factor eEF1A and its bacterial counterpart EF1A (EF-Tu), which are known to form a ternary complex with GTP and aminoacylated elongator tRNAs (Krab & Parmeggiani, 1998).

In the cell, e/aIF2 acts as a molecular switch that cycles between inactive (GDP-bound) and active (GTP-bound) states, passing through an intermediate nucleotide-free state. The crystal structures of aIF2γ in nucleotide-free (Schmitt *et al.*, 2002; Roll-Mecak *et al.*, 2004; Sokabe *et al.*, 2006; Nikonov *et al.*, 2007), GDP-bound (Schmitt *et al.*, 2002; Sokabe *et al.*, 2006; Nikonov *et al.*, 2007; Yatime *et al.*, 2007) and GDPNP-bound (a nonhydrolyzable GTP analogue) states (Schmitt *et al.*, 2002; Yatime *et al.*, 2006) demonstrate a conformation with a three-domain arrangement similar to that of EF-Tu in complex with GDPNP (Berchtold *et al.*, 1993). In the case of EF-Tu, however, an active GTP-bound ON state and an inactive GDP-bound OFF state (Berchtold *et al.*, 1993; Kjeldgaard *et al.*, 1993; Song *et al.*, 1999) with two different conformations, EF-Tu–GDPNP and EF-Tu–GDP, have been observed. The conformational changes involve drastic relative motions between domain I (the G domain) and domains II and III of the protein, as well as concerted motions of two flexible regions of the G domain called switch 1 and switch 2. The relative orientations of domains II and III are very similar

in the two EF-Tu states, and these two domains can be considered as a single structural unit. The structure of EF-Tu in the nucleotide-free state is unknown. Domain rearrangements and conformational changes of switch regions corresponding to the nucleotide-free and nucleotide-bound states of aIF2γ have also been observed (Schmitt *et al.*, 2002; Roll-Mecak *et al.*, 2004; Sokabe *et al.*, 2006).

In eukaryotes, the nucleotide state of eIF2 is regulated with the help of several initiation factors. In particular, hydrolysis of eIF2-bound GTP is controlled by eIF5, a GTPase-activating protein (GAP). Previously, it was thought that the action of eIF5 was triggered by recognition of the start codon. However, detailed biochemical experiments show that this protein is able to promote GTP hydrolysis by eIF2 in the absence of mRNA, producing the eIF2–GDP–P_i complex. The initiation factor eIF1 blocks the release of inorganic phosphate (P_i) from the ternary complex on the ribosome (Algire *et al.*, 2005). Upon start-codon recognition, eIF1 is displaced from the P site of the ribosome, leading to release of P_i and dissociation of eIF2–GDP. The tightly bound GDP must be released from eIF2 so that eIF2 can be reactivated by the binding of GTP. The dissociation of GDP from eIF2 is catalyzed by the nucleotide exchange factor (GEF) eIF2B (Kyrpides & Woese, 1998). In archaea, eIF5 and eIF2B have no orthologues, and GTP hydrolysis and the recycling of aIF2–GDP into aIF2–GTP should be spontaneous (Schmitt *et al.*, 2002; Pedullà *et al.*, 2005).

The conformational transitions that take place in aIF2 upon switching between its active and inactive states have been investigated using molecular-dynamics (MD) simulations (Satpati & Simonson, 2012). The authors used the known crystal structures of aIF2γ from *Sulfolobus solfataricus* (Sso aIF2γ) to model the aIF2γ–GTP ON state and the aIF2γ–GDP OFF state, whereas the aIF2γ–GDP–P_i ON state was modelled by breaking the bond between the β and γ phosphates in the aIF2γ–GTP structure and allowing the product to gently relax. The MD structure of aIF2γ–GDP–P_i demonstrated some evident changes in the conformation of the nucleotide-binding pocket and a new Mg^{2+}-ion position close to that of the γ phosphate in the aIF2$\alpha\gamma$ heterodimer (Yatime *et al.*, 2006). In contrast to eIF2–GDP–P_i in the eukaryotic ternary complex (Algire *et al.*, 2005), the archaeal post-hydrolysis complex, aIF2γ–GDP–P_i, appears to be very unstable (Satpati & Simonson, 2012).

A structure that possibly indicates the state of Sso aIF2 one step after GTP hydrolysis into GDP and P_i and one step before pairing of tRNA with the start codon has been obtained by Yatime *et al.* (2007). In this low-resolution (3.2 Å) GDP-bound form of Sso aIF2$\alpha3\beta\gamma$ the conformation of the switch 2 region and the domain arrangement of aIF2γ corresponded to the typical ON conformation. No Mg^{2+} ion was found in the nucleotide-binding pocket. Rather, the position expected for an Mg^{2+} ion was occupied by the side chain of His37. The conformation of switch 1 corresponded neither to the OFF state nor to the ON state. The stability of this intermediate state was maintained by a ligand, possibly a phosphate ion, which interacted with both switch regions.

Here, we report four high-resolution crystal structures of wild-type aIF2γ and its mutants from *S. solfataricus* (Sso aIF2γ): aIF2γ–GDPCP (a nonhydrolyzable GTP analogue), aIF2γ–GDP–formate (in which a formate ion possibly mimics P_i), aIF2γ–GDP and nucleotide-free aIF2γ. The structures demonstrate the conformational transitions that take place in this protein upon nucleotide binding and switching between its different states. In the case of aIF2γ–GDPCP the mutant form of aIF2γ with deletion of the central part of switch 1 was used for crystallization; the structure of this mutant did not differ from that of the wild-type protein and the deletion did not preclude aIF2γ–GDPCP complex formation. It should be emphasized that the aIF2γ–GDP–formate and aIF2γ–GDP crystals were obtained by co-crystallization of aIF2γ in the presence of purified GTP, but GDP was found in the nucleotide-binding pockets of both complexes. Our data demonstrate that sodium formate at high concentrations is able to stabilize the switch regions in positions characteristic of the ON state of aIF2γ and EF-Tu. Nucleotide-free Sso aIF2γ shows a conformation closer to the ON state, in contrast to other known nucleotide-free aIF2γ structures.

2. Materials and methods

2.1. Overproduction and purification of the mutant forms of *S. solfataricus* aIF2γ

In our investigations, three mutant structures were used. A very flexible central part of switch 1 was deleted to evaluate its role in the binding of nucleotides. Fortunately, these deletions and substitutions in the noncanonical nucleotide-binding pocket resulted in higher resolution diffraction data. Deletion of the sequences corresponding to residues 41–45 and 37–47 (switch 1) and the replacement of residues Phe221/Lys225/Arg280 of aIF2γ by alanines in aIF2γ were achieved by site-directed mutagenesis of pET-11d-γ using the QuikChange method (Stratagene). The mutant proteins were overproduced and purified as described previously (Nikonov *et al.*, 2007).

2.2. GTP purification

5 mg GTP (Sigma) dissolved in 500 µl buffer (20 m*M* Tris–HCl pH 7.5) was loaded onto a Mono Q column (1 ml) equilibrated with the same buffer. The column was washed with 10 ml of the same buffer, and a 30 ml linear gradient of NaCl concentration (0–1 *M*) in the same buffer was used for elution of the nucleotide. The optical density of fractions was estimated at 220, 260 and 280 nm. Peak fractions were tested by thin-layer ion-exchange chromatography on plates with PEI-cellulose (Merck) in 0.1 *M* Tris–HCl pH 8.0 with 0.5 *M* LiCl in a glass camera during 15 min. Pure GTP and GDP were used as markers. Spots were detected using a UV lamp.

2.3. Crystallization of the mutant forms of Sso aIF2γ with and without nucleotides

Crystallization trials were performed at 28°C by the hanging-drop vapour-diffusion technique using mutant Sso aIF2γ protein at a concentration of 50 mg ml^{-1} in buffer

Table 1
Data-collection and refinement statistics.

Values in parentheses are for the highest resolution shell.

Structure	aIF2γ–GDPCP	aIF2γ–GDP–formate	aIF2γ–GDP	aIF2γ
Data collection				
Source	BESSY BL14.1	BESSY BL14.1	Bruker AXS MICROSTAR	BESSY BL14.1
Wavelength (Å)	0.91841	0.91841	1.54179	0.91841
Space group	*I*23	*R*32	$P2_1$	$P3_121$
Unit-cell parameters				
a (Å)	186.89	142.86	86.05	95.81
b (Å)	186.89	142.86	106.55	95.81
c (Å)	186.89	218.41	156.30	165.24
α (°)	90.00	90.00	90.00	90.00
β (°)	90.00	90.00	90.63	90.00
γ (°)	90.00	120.00	90.00	120.00
Resolution (Å)	19.70–2.00 (2.10–2.00)	45.73–2.25 (2.35–2.25)	19.81–2.60 (2.70–2.60)	47.91–2.15 (2.25–2.15)
Observed reflections	365256 (48649)	452939 (54385)	284650 (25550)	284714 (35794)
Unique reflections	72719 (9781)	40715 (4843)	84101 (8374)	48518 (6088)
Completeness (%)	99.6 (98.6)	99.8 (99.0)	96.7 (90.5)	99.9 (99.7)
Multiplicity	5.01 (4.90)	11.10 (11.12)	3.27 (2.76)	5.86 (5.87)
$\langle I/\sigma(I)\rangle$	12.77 (2.73)	19.35 (4.47)	14.29 (1.93)	18.01 (3.83)
$R_{\rm merge}$ (%)	10.76 (49.07)	8.41 (42.12)	5.60 (44.40)	5.68 (37.40)
Refinement				
Resolution range (Å)	19.70–2.00 (2.03–2.00)	45.73–2.25 (2.31–2.25)	19.81–2.60 (2.63–2.60)	47.91–2.15 (2.19–2.15)
$R_{\rm work}/R_{\rm free}$† (%)	16.00/18.45 (25.09/29.33)	15.20/18.20 (22.04/27.67)	23.40/28.60 (33.76/37.58)	18.80/22.80 (25.75/31.12)
No. of atoms				
Protein	3221	3250	18901	3080
Ligands	147	121	180	148
Water	654	437	363	255
R.m.s.d.				
Bond lengths (Å)	0.006	0.006	0.005	0.007
Bond angles (°)	1.143	1.075	0.965	1.127
B factor (Å^2)	19.97	36.94	54.60	42.54

† $R_{\rm free}$ factors were calculated for randomly selected test sets of 5.0% of the reflections that were not used in the refinement.

consisting of 50 m*M* Tris–HCl pH 7.5, 400 m*M* NaCl, 10 m*M* β-mercaptoethanol. The protein was mixed with reservoir solution in equal amounts. A reservoir solution consisting of 100 m*M* sodium cacodylate pH 6.5, 4 *M* sodium formate was used for the crystallization of Sso aIF2γ (Δ37–47) with GDPCP and of Sso aIF2γ (F221A/K225A/R280A) with GTP. Commercial preparations of nucleotides (GDPCP from Jena Bioscience and additionally purified GTP from Sigma) were added to the drop to a final concentration about 5 m*M*. Crystals of Sso aIF2γ(Δ41–45) in a nucleotide-free form were obtained using a reservoir solution consisting of 50 m*M* Na HEPES pH 7.0, 50 m*M* $MgSO_4$, 1.6 *M* Li_2SO_4. Cryoprotection of the crystals was achieved by adding ethylene glycol to the reservoir solution to a final concentration of 15%(*v*/*v*).

2.4. Crystallization of wild-type Sso aIF2γ in complex with GDP

Crystallization trials were performed at 22°C by the hanging-drop diffusion technique using Sso aIF2γ protein at a concentration of 25 mg ml^{-1} in a buffer consisting of 10 m*M* Tris–HCl pH 7.5, 100 m*M* NaCl, 100 m*M* KCl, 10 m*M* $MgCl_2$, 10 m*M* β-mercaptoethanol. The protein solution (3 µl) was mixed with 0.5 µl 6 m*M* purified GTP pH 7.5 and 2 µl reservoir solution consisting of 100 m*M* Tris–HCl pH 7.5, 180 m*M* KBr, 13% PEG 4000 (Clear Strategy Screen 1 solution No. 10). Crystals of Sso aIF2γ–GDP were obtained within 7 d. Cryoprotection of the crystals was achieved by adding ethylene glycol to the reservoir solution to a final concentration of 15%(*v*/*v*).

2.5. Data collection, structure determination and refinement

X-ray diffraction data were collected using synchrotron radiation on the BL14.1 HZB beamline at BESSY, Berlin, Germany with an MX-225 CCD detector (Rayonics, Evanston, USA) and using a rotating-anode radiation source (Bruker AXS MICROSTAR) with a CCD detector (Bruker PLATINUM 135) at RAS, Pushchino, Russia.

The data were processed and merged with the *XDS* program suite (Kabsch, 1993) and the *PROTEUM*^{plus} software package (Bruker AXS). A molecular-replacement solution was obtained with *Phaser* (Storoni *et al.*, 2004). To find unique positions of the γ subunits in the aIF2γ–GDPCP and aIF2γ–GDP–formate structures, the previously determined structure of aIF2γ–GDP (PDB entry 2pmd; Nikonov *et al.*, 2007) was used as a search model. Nucleotides, ions and water were excluded from the model. The crystal of the aIF2γ–GDP complex belonged to space group $P2_1$ and contained six molecules in the asymmetric unit. This fact, together with the high flexibility of the molecule, led to difficulties in finding a search model. Only the G subunit of one of the four copies of the aIF2 trimer (PDB entry 3cw2; Stolboushkina *et al.*, 2008) could be used. The structure of nucleotide-free aIF2γ was solved using the nucleotide-free form of aIF2 from *Pyrococcus*

abyssi (PDB entry 1kk0; Schmitt *et al.*, 2002) as a search model.

The models were subjected to several rounds of computational refinement and map calculation with *PHENIX* (Adams *et al.*, 2002) and manual model inspection and modification with *Coot* (Emsley *et al.*, 2010). The data-collection and refinement statistics are summarized in Table 1. The model bias existing in the initial molecular-replacement solutions was tackled using composite OMIT cross-validated σ_A-weighted maps as implemented in *CNS* (Brünger *et al.*, 1998).

3. Results

3.1. Overall description of the structures

3.1.1. The aIF2γ–GDPCP complex. In all known structures of aIF2γ the switch 2 region can adopt OFF or ON conformations only. In contrast, the central part of the switch 1 region displays irregular conformations that are presumably influenced by crystal packing and not by the nature of the bound nucleotide (Nikonov *et al.*, 2007; Yatime *et al.*, 2007; Stolboushkina *et al.*, 2008). Because switch 1 showed a conformation in the structure of the aIF2$\alpha\gamma$ heterodimer from *S. solfataricus* bound to GDPNP that was similar to that of EF-Tu–GDPNP, it was suggested that this switch participates in the binding of GTP (Yatime *et al.*, 2006). However, this function of switch 1 was not evident. Therefore, we deleted the central part of switch 1 (amino-acid residues 37–47) in aIF2γ and cocrystallized this mutant with GDPCP. Additionally, these crystals demonstrate a higher resolution in comparison with the aIF2$\alpha\gamma$–GDPNP complex (Yatime *et al.*, 2006).

The structure of aIF2γ–GDPCP from *S. solfataricus* (subsequently indicated as structure S1) has been solved at 2.0 Å resolution. A stereoview of the structure is shown in Fig. 1 and the amino-acid sequence of the γ subunit is shown in Supplementary Fig. S1[1]. The mutant structure clearly demonstrates the presence of GDPCP–Mg^{2+} in the nucleotide-binding pocket and a lack of significant interactions (apart from a hydrogen bond that is accessible to the solvent formed by the NZ atom of Lys48 and the O3G atom of GDPCP) between truncated switch 1 and GDPCP. This structure and the structure of aIF2$\alpha\gamma$–GDPNP previously determined at 3.0 Å resolution (Yatime *et al.*, 2006) are closely similar and can be superimposed with an r.m.s.d. of 0.610 Å for 94% compared C^{α} atoms. The positions of domains II and III relative to domain G are identical in both structures.

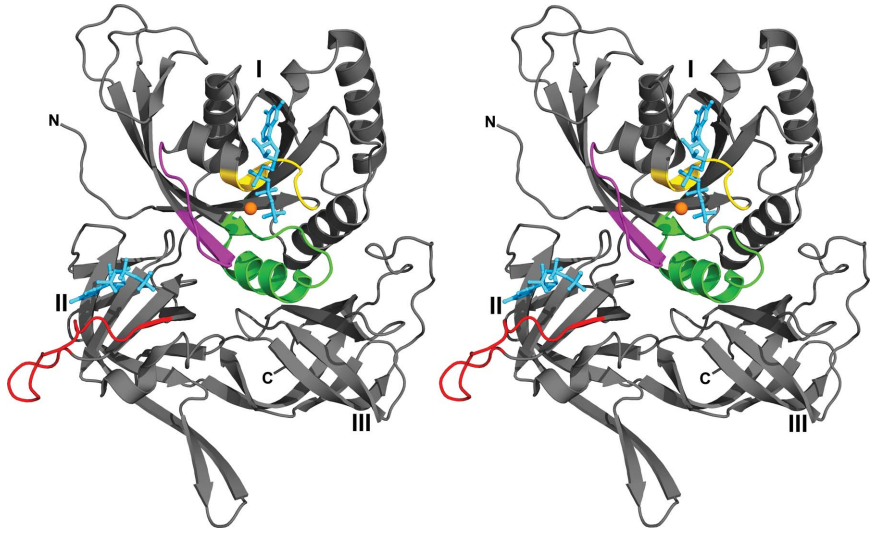

Figure 1
A stereoview of *S. solfataricus* aIF2γ–GDPCP. The γL1 loop, P loop and the switch 1 and switch 2 regions are shown in red, yellow, magenta and green, respectively. The Mg^{2+} ion is shown as an orange ball. The GDPCP molecules are shown in cyan. Domains are numbered with roman numerals.

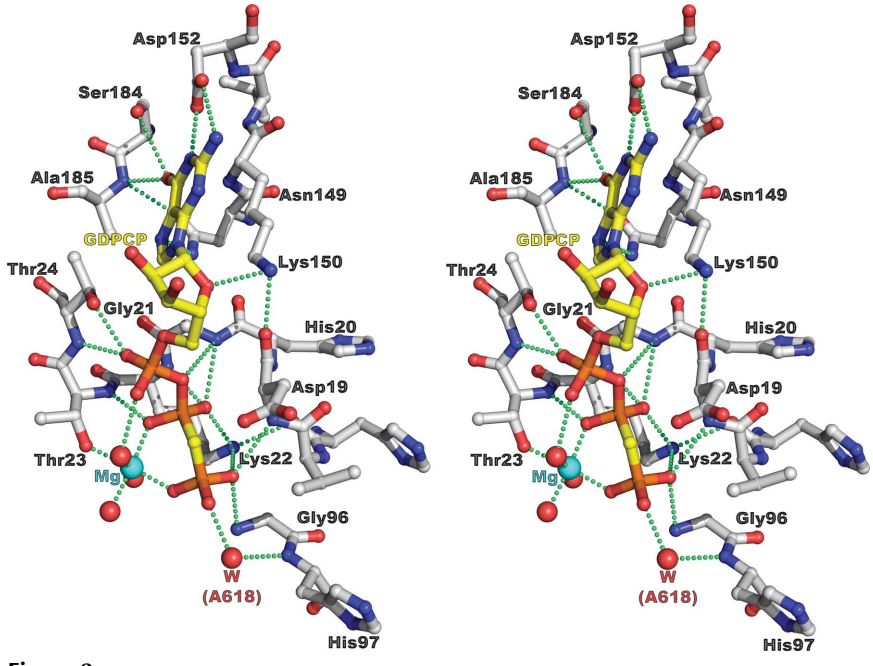

Figure 2
The nucleotide-binding pocket of the aIF2γ–GDPCP complex. The side chains of Asp152 and Ser184 mimic the interactions characteristic of a canonical G–C pair. The P loop (residues 19–23) forms a bed for the α-phosphate and β-phosphate groups. The O3G γ-phosphate O atom forms hydrogen bonds to the main-chain N atom of Gly96 and the NZ atom of Lys22. The C3B β–γ bridge atom (O3B in GTP) forms a hydrogen bond to the main-chain N atom of Asp19. The Mg^{2+} ion is coordinated by the O2B and O2G atoms of GDPCP, the OG1 atom of Thr23, the NZ atom of Lys48 and two water molecules. Water molecule A618 occupies a position close to that required for nucleophilic attack.

[1] Supporting information has been deposited in the IUCr electronic archive (Reference: MN5043).

The nucleotide-binding pocket of aIF2γ is built up from the P loop (residues 18–23), the switch 2 region (residues 93–113), loop β6–α4 (residues 149–152) and loop β7–α5 (residues 185–187) (Fig. 2 and Supplementary Fig. S1). The two latter regions surround the base of the nucleotide. The side chains of Asp152 and Ser184 mimic the interactions characteristic of a canonic G–C pair. These interactions are conserved in all known G-protein structures and ensure the specificity for guanine nucleotides (Simonetti *et al.*, 2013).

It is interesting to note that except for the switch 1 region, superposition of C^{α} atoms of the nucleotide-binding pockets of aIF2γ and *Thermus thermophilus* EF-Tu (Tth EF-Tu; Berchtold *et al.*, 1993), both in the ON state, produces an r.m.s. deviation of 0.498 Å, thus demonstrating the high stability of this region in the superfamily of ribosomal GTP-binding proteins. The positions of GDPCP, GDPNP and Mg^{2+} are very similar in these aIF2γ and EF-Tu structures. Moreover, a hydrogen bond that is crucial for GTP hydrolysis by elongation factor EF-Tu between the main-chain amide N atom of Gly96 (Sso aIF2 numbering) and the γ-phosphate (Knudsen *et al.*, 2001) is found in the S1 structure (Fig. 2) and in the structure of aIF2$\alpha\gamma$–GDPNP (Yatime *et al.*, 2006). The identity of interactions between the protein and nucleotide in the aIF2γ structure with a truncated switch 1 region, the wild-type (Yatime *et al.*, 2006) protein and EF-Tu (Berchtold *et al.*, 1993) shows that at least the central part of the switch 1 region of the γ subunit (amino-acid residues 37–47) does not take part in the binding of the GTP analogues.

Similar to the previously determined aIF2γ–GDP complex (Nikonov *et al.*, 2007), the second GDPCP molecule was also found in the noncanonical nucleotide-binding pocket of the S1 structure. In both structures, the locations of the bases and riboses of the extra G nucleotides were identical, whereas the locations of the phosphate moieties were different. Superposition of domain II of the S1 structure on that of the ternary complex (Stolboushkina *et al.*, 2013) showed that the noncanonical nucleotide-binding pocket possibly corresponds to the positioning of the G2 nucleotide base of the initiator tRNA.

3.1.2. The aIF2γ–GDP–formate complex. The wild-type aIF2γ–GDP–formate structure in the ON state has been solved at 2.4 Å resolution, whereas this complex with point mutations (F221A, K225A and R280A) in the additional nucleotide-binding site (Nikonov *et al.*, 2007) produced diffraction data to 2.0 Å resolution, but the real resolution was not better than 2.25 Å (because the data set was not complete beyond a Bragg spacing of 2.25 Å). Both complexes were obtained by co-crystallization of aIF2γ with purified GTP, but GDP was found in canonical nucleotide-binding pockets of the wild-type and mutant structures (the crystallization conditions were identical). Apparently, GTP was hydrolyzed rather quickly in the crystallization solution and the aIF2γ–GDP complex was crystallized. These structures can be superimposed with an r.m.s.d. of 0.192 Å for 98% compared C^{α} atoms, and hereafter we will consider the structure formed by the mutant protein only (structure S2). A stereoview of this structure is shown in Fig. 3.

The superposition of C^{α} atoms of the canonical nucleotide-binding pockets of the S1 and S2 structures produces an r.m.s. deviation of 0.391 Å; the domain arrangements in these structures are also very similar (with an r.m.s.d. of 0.734 Å for 90.8% compared C^{α} atoms). The positions of the bases and the α-phosphate and β-phosphate groups of the nucleotides are identical in both structures. In the S2 structure, the Mg^{2+} ion is shifted about 0.5 Å towards the α-phosphate relative to its position in the S1 structure and is coordinated by O1B of GDP, OG1 of Thr23 and four water molecules (Fig. 4). The G domain of the S2 structure contains the full-length switch 1 region, with the α-helix formed by amino-acid residues 36–44. Residues 31–35 form a likeness of the extreme β-strand of the seven-stranded β-sheet. A similar α-helix and β-strand also exist in the corresponding switch 1 region of the EF-Tu–GDPNP complex. Based on these data, it is possible to conclude that the S2 structure demonstrates the ON state for all functionally important labile regions of Sso aIF2γ: the P loop, switch 1 and switch 2 regions.

Analysis of the S2 structure reveals the formate ion which holds switch 1 and switch 2 in the ON state (Fig. 4, Supplementary Fig. S2). The O atoms of this ion form hydrogen bonds to the main-chain amide N atoms of Gly96 and His97 of switch 2 and the main-chain N atom of Thr46 of switch 1. Additionally, the formate ion interacts through

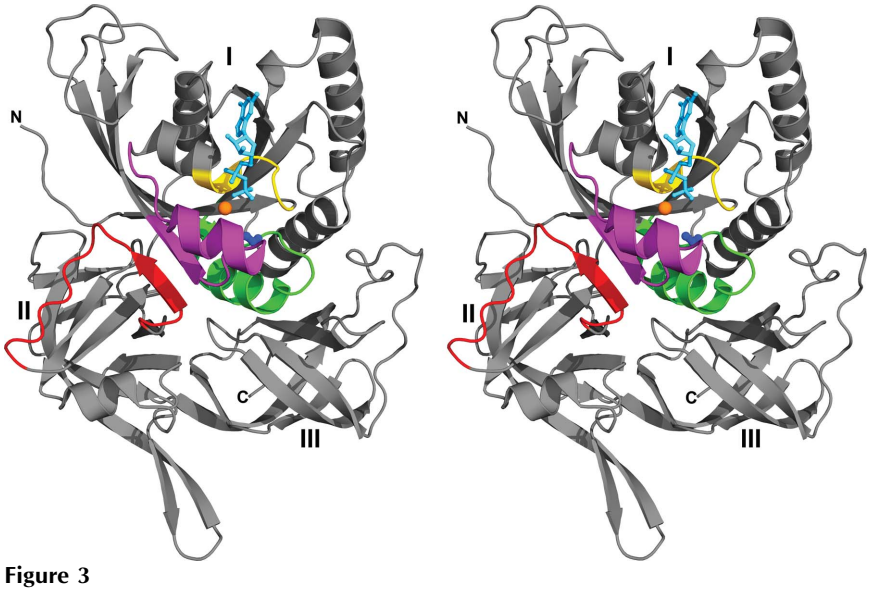

Figure 3
A stereoview of *S. solfataricus* aIF2γ–GDP–formate. The γL1 loop, P loop and the switch 1 and switch 2 regions are shown in red, yellow, magenta and green, respectively. The GDP molecule is shown in cyan. The Mg^{2+} ion is shown as an orange ball. The formate ion (shown in marine) acts as a switch 1–switch 2 clip through its O atoms. The central part of the switch 1 region forms an α-helix; its C-terminus forms a likeness of the extreme β-strand of the β-sheet of domain I. The γL1 loop and loop α6–β16 (residues 308–313) drastically change their conformations in comparison with those shown in Fig. 1.

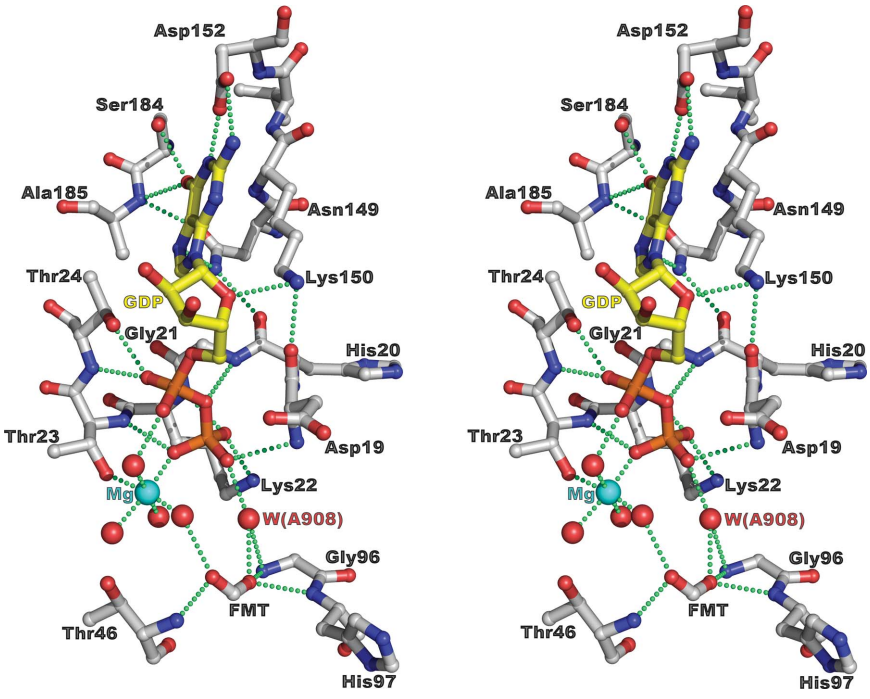

Figure 4
The nucleotide-binding pocket of the aIF2γ–GDP–formate complex. The position of GDP is identical to that observed in the S1 structure. The Mg^{2+} ion is shifted towards the α-phosphate and is coordinated by the O1B atom of GDP, the OG1 atom of Thr23 and four water molecules. The O3B β–γ bridge atom forms a hydrogen bond to the main-chain N atom of Asp19. Water molecule W(A908) occupies a position close to that occupied by the O3G atom of GDPCP in the S1 structure. The formate ion fastens switch 2 with switch 1 and holds them in the ON state. Two of its O atoms form hydrogen bonds to the main-chain amide groups of Gly96 and Thr46, respectively.

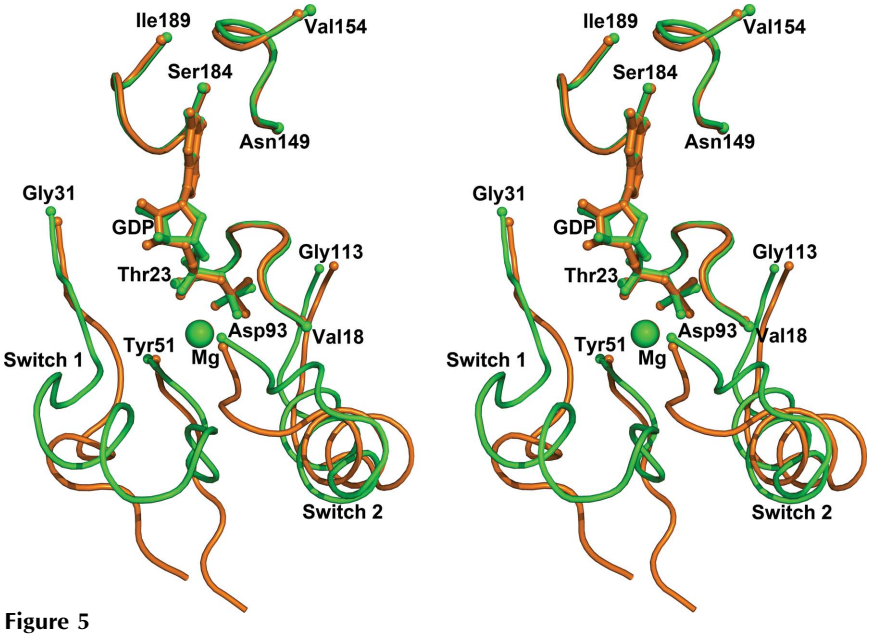

Figure 5
Superposition of the nucleotide-binding pockets of the S2 (green) and S3 (orange) structures demonstrating the ON and OFF states, respectively. In both structures the positioning of the GDP and Mg^{2+} groups is very close. The P loop (18–23), loop β6–α4 (149–154) and loop β7–α5 (184–189) retain their conformations and positions, whereas switch 1 and switch 2 have different conformations in the active and inactive states of aIF2γ. In the OFF state, the C-terminal part of switch 2 makes up a bulge protruding into the contact region between domain I and domains II and III, thus changing the relief of the G-domain surface in the interface region.

water molecules with the Mg^{2+} ion, β-phosphate and Lys22 of the P loop. This ion occupies a position close to that occupied by P_i in the aIF2α3$\beta\gamma$–GDP–P_i structure (Yatime *et al.*, 2007). However, the formate ion connects the NH group of Gly96 of switch 2 to the C-terminal part of switch 1, whereas P_i connects the same group of switch 2 to the N-terminal part of switch 1 *via* a water molecule (Supplementary Fig. S3) and is located on the surface of the protein. All O atoms of P_i are accessible to the solvent and it can easily be substituted by water molecules in solution. Based on these data, it is conceivable that the formate ion mimics the possible P_i position that comes before the position of P_i in the aIF2α3$\beta\gamma$–GDP–P_i structure.

To resolve the role of the formate ion in the conformational transition of aIF2γ more precisely, we cocrystallized aIF2γ with pure GDP in the presence of 4 *M* sodium formate and solved this structure. This structure was completely identical to the S2 structure and the formate ion occupied an identical position (data not shown) in both structures. Consequently, the presence of GTP in the original mother liquor did not influence the state of aIF2γ, but the presence of highly concentrated formate in the crystallization solution stabilized the GDP-bound aIF2γ in the ON state.

Large changes were found in domain II of the S2 structure. Loop γL1 (residues 220–234) and loop α6–β16 (residues 308–313) changed their conformation dramatically in comparison with all known aIF2γ structures. Loop γL1 is shifted in the direction of domain I and its residues 222–225 form a β-strand parallel to strand β2 of this domain. Loop α6–β16 is shifted towards β-hairpin β10–β11 and forms an additional three-stranded antiparallel β-sheet of domain II (Fig. 3 and Supplementary Fig. S4). Notice that both of these loops in their common conformations make up the protein–protein interface between the γ and α subunits of aIF2 (Yatime *et al.*, 2006). The new position of loops γL1 and α6–β16 disrupts complementarity between domain 3 of the α subunit and the γ subunit and eliminates the possibility of $\alpha\gamma$ heterodimer formation. Thus, it is possible to suggest that these loops could also act as switches.

3.1.3. The aIF2γ–GDP complex. The structure of the aIF2γ–GDP complex (structure S3) has been determined at 2.6 Å

resolution. The asymmetric unit of the crystal contains six molecules with slightly different positions of small helices and short β-strands in their long loops. The molecules in the asymmetric unit of the crystal are packed into two trimers which are related by a noncrystallographic twofold translation axis parallel to the *b* axis of the cell. The switch 1 region and the γL1 loop are both positioned within the inner hole of the trimer and have different conformations in the different monomers. The central parts of these loops (residues 37–44 and 228–230) show poor electron density in all six molecules. After exclusion of the switch 1 region and the γL1 loop, pairwise superposition of all of the monomers yielded an r.m.s. deviation for the remaining 378 C^{α} atoms of around 0.7 Å. This shows that the relative orientation of the domains in all of the complexes is similar.

Similar to the S2 structure, the crystals of this complex were obtained by co-crystallization of aIF2γ with purified GTP, but GDP–Mg^{2+} was found in the canonical nucleotide-binding pockets of all six molecules. Thus, similar to the previous case, GTP could be spontaneously hydrolyzed in solution during crystallization. The N-terminal parts of the switch 2 regions in all six aIF2γ–GDP molecules in the asymmetric unit of the crystal adopt a helical conformation (Fig. 5). The C-terminal residues 107–109 of this switch makes up a bulge that protrudes from the core of the G domain into the space between this domain and domain III, forming an interdomain parallel β-sheet with loop β17–β18 of domain III and initiating the new domain arrangement.

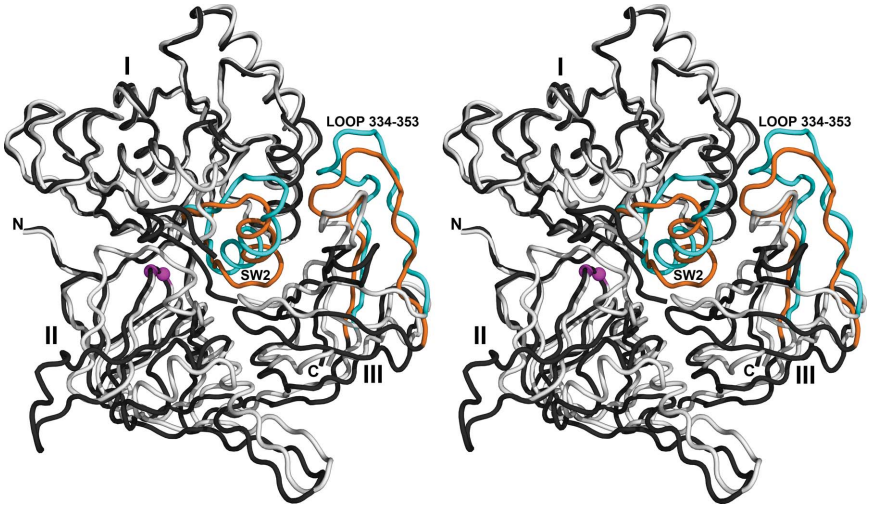

Figure 6
Domain displacement in aIF2γ during transition from the active to the inactive state. The G domains of the S2 and S3 structures are superimposed. Domains are numbered with roman numerals and shown in dark and light grey for the OFF and ON states, respectively. In the OFF state, switch 2 and loop 334–353 are shown in orange. The same elements in the ON state are shown in blue. Upon transition from the OFF state to the ON state, domains II and III rotate about an axis approximately coincident with a line connecting the C^{α} atoms of residues 292–293 (magenta spheres) approaching domain G.

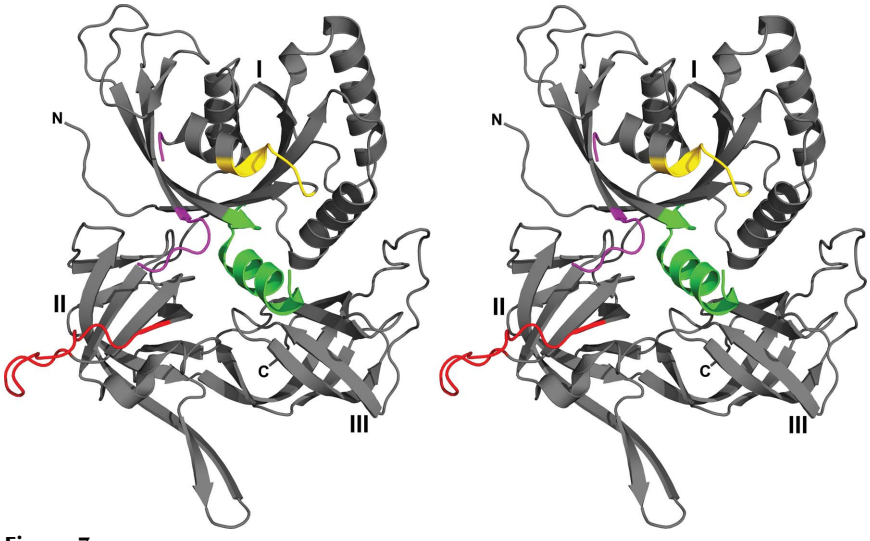

Figure 7
Stereoview of *S. solfataricus* aIF2γ. The γL1 loop, P loop and the switch 1 and switch 2 regions are shown in red, yellow, magenta and green, respectively. The P loop and the N-terminal part of switch 2 change their conformations (residues 96–98 of switch 2 are not visible in the structure). The conformation of switch 2 corresponds to the ON state.

Monomer *A* of the S3 structure and aIF2γ of the previously determined structure of aIF2α3β1γ–GDP (Yatime *et al.*, 2007) in the OFF state are closely similar and can be superimposed with an r.m.s.d. of 0.843 Å for 86% compared C^{α} atoms. A similar result was obtained on superposition of monomer *A* of the S3 structure and the aIF2γ–GDP complex from *P. abyssi* (Pab aIF2γ) solved at 1.9 Å resolution (Schmitt *et al.*, 2002). In contrast, the superposition of this monomer and aIF2γ in the ON state from the aIF2$\alpha\gamma$ heterodimer (Yatime *et al.*, 2006) produced an r.m.s. deviation of 1.83 Å for the same set of C^{α} atoms. These results unambiguously demonstrate the OFF state of the S3 structure.

The comparison of the aIF2γ structures in the OFF and ON states shows a clearly visible displacement of domains II and III relative to domain G; these domains are rotated by about 10–15° around an axis approximately coincident with a line connecting the C^{α} atoms of residues 292–293 of domain II (Fig. 6). This confirms that Sso aIF2 acts similarly to other GTPases (Berchtold *et al.*, 1993; Song *et al.*, 1999; Vetter & Wittinghofer, 2001; Liljas *et al.*, 1995); aIF2γ also has a different arrangement of domains II and III relative to domain G in the ON and OFF states. However, the domain reorganization is not as dramatic as that observed in the EF-Tu–GDPNP and EF-Tu–GDP structures.

At the same time, the switch 1 regions of either of the two copies of aIF2γ–GDP can be superimposed on each other with an r.m.s. deviation within the range 2.3–4.1 Å.

Only small parts of switch 1, which include amino-acid residues 31–34 and 49–51, appear to retain their conformation in the different monomers. Comparison with the conformation of switch 1 regions in other known aIF2γ structures indicates that this region generally retains its mobility in all observed states of aIF2γ and may adopt any conformation dictated by crystal packing or other factors, independently of the type of nucleotide bound. Moreover, its central part plays no role in either GTP or GDP binding.

3.1.4. Nucleotide-free aIF2γ. Upon going from the GDP-bound to the GTP-bound form, the GTPase passes through the nucleotide-free form. This form is unknown for EF-Tu. However, several structures of nucleotide-free aIF2γ from different organisms are available (Schmitt *et al.*, 2002; Roll-Mecak *et al.*, 2004; Sokabe *et al.*, 2006). Some years ago, the structure of free aIF2γ from *S. solfataricus* was solved by our group at 2.9 Å resolution (Nikonov *et al.*, 2007). The conformation and location of the switch 2 region in this structure dramatically differed from that observed in all other nucleotide-free aIF2γ structures, which demonstrated the classical OFF form. To prove that this was not an artifact, the structure of a mutant Sso aIF2γ (structure S4) was solved in a nucleotide-free form (Fig. 7). In this structure, the deletion of amino-acid residues 41–45 resulted in higher resolution (2.15 Å) diffraction data. The two nucleotide-free Sso aIF2γ forms were closely similar and could be superimposed with an r.m.s.d. of 0.512 Å for 87% compared C^{α} atoms. The domain arrangement and location of the N- and C-terminal parts of switch 1 (residues 31–34 and 49–51, respectively) were identical in both structures. Differences were only found in the N-terminus of the P loop (residues 18–20) and the switch 2 region (residues 93–101). Residues 96–98 were not visible in the S4 structure. In the P loop, the conformational changes emerged as a result of the disruption of two hydrogen bonds from the main-chain O atoms of Asp19 and His20 to the NZ atom of Lys150 and the ND atom of Asn149, respectively, which stabilized the P loop in the nucleotide-bound forms. The OFF conformation of switch 2 is stabilized by hydrogen bonds formed by the main-chain O atoms of Ala94 and Pro95 to water molecules coordinating the Mg^{2+} ion, whereas the ON conformation of this switch is stabilized by the hydrogen bond formed by the main-chain O atom of Gly96 to the O atom of the γ-phosphate. All of these hydrogen bonds are nucleotide-dependent.

In contrast to the nucleotide-free forms of aIF2γ from *P. abyssi* (Schmitt *et al.*, 2002), *Methanocaldococcus jannaschii* (Roll-Mecak *et al.*, 2004) and *P. furiosus* (Sokabe *et al.*, 2006), in the nucleotide-free forms of Sso aIF2γ the position of the switch 2 helix is shifted from spanning residues 97–107 corresponding to the GDP-bound form to residues 100–110 corresponding to the GTP-bound form. The superposition of domain I of the S4 structure on those of the S1 and S3 structures shows that in the nucleotide-free form of aIF2γ domains II and III also demonstrate a position relative to domain I which is closer to the ON state (Supplementary Fig. S5). In summary, we can say that the nucleotide-free form of Sso aIF2γ is probably preferred to the binding of GTP. This possibly explains the similar affinity for GTP and GDP obtained in Sso aIF2 activity assays (Pedullà *et al.*, 2005).

4. Discussion

4.1. Hydrolysis of GTP and GDP/GTP exchange in archaea

A comparison of the canonical nucleotide-binding pockets of the S1, S2 and S3 complexes shows that with the exception of the switch regions they have very stable conformations which are identical in both the active and inactive states of aIF2γ. Identical structures of the pocket are observed in the EF-Tu–GDPNP (Berchtold *et al.*, 1993) and EF-Tu–GDP complexes (Polekhina *et al.*, 1996; Song *et al.*, 1999). A comparison (Supplementary Fig. S6) shows that the base, ribose and α- and β-phosphates of G nucleotides occupy the same positions in aIF2γ and EF-Tu in both the ON and OFF states. The Mg^{2+} ion can move slightly, but its displacement is not more than 1.0 Å. Previously, there was reason to believe that the nucleotide-binding pocket of e/aIF2γ is distinct from that in the G domain of monomeric bacterial IF2 (Kyrpides & Woese, 1998). However, the crystal structure of the protein core of translation initiation factor 2 from *T. thermophilus* in the nucleotide-free, GTP-bound and GDP-bound forms (Simonetti *et al.*, 2013) showed that the nucleotide-binding pocket of IF2 is identical to that of aIF2γ and other ribosomal GTPases.

At the same time, it is known that guanine nucleotides bind with a dissociation constant of 10^{-8}–10^{-9} *M* to EF-Tu from *T. thermophilus* (Arai *et al.*, 1978), while the γ subunit and intact aIF2 from *S. solfataricus* have a more limited affinity for GDP and GTP ($\sim 4 \times 10^{-7}$ *M*; Pedullà *et al.*, 2005). Moreover, in *in vitro* experiments at the optimal growth temperature for *S. solfataricus* aIF2, radiolabelled GDP can be replaced by either GDP or GTP at a comparable rate and nucleotide exchange was complete within 4 min (Pedullà *et al.*, 2005). To account for this phenomenon, we compared the conformations of the switch 1 regions in the S2 and EF-Tu structures. It turned out that the nucleotide-binding pocket of aIF2γ is open and accessible to the solvent, in contrast to the pocket of EF-Tu, which is closed by Tyr47 and Ile61 (Trp33 and Met45 in Sso aIF2γ).

The catalysis of GTP hydrolysis in ribosomal GTPases requires an invariant histidine (His97 in Sso aIF2γ and His85 in EF-Tu from *T. thermophilus*) that acts as a general base, abstracting a proton from a water molecule for inline attack on the γ-phosphate of GTP (Berchtold *et al.*, 1993; Kjeldgaard *et al.*, 1993; Li & Zhang, 2004; Simonetti *et al.*, 2013). In the S1 structure, the nucleophilic water molecule A618 (the analogue of W411 in EF-Tu–GDPNP from *T. thermophilus*) is close to the γ-phosphate but is not aligned correctly for catalysis (Fig. 2). Premature GTP hydrolysis in EF-Tu is thought to be prevented by a closed 'hydrophobic gate', which restricts access of the catalytically important histidine to the catalytic water molecule (Berchtold *et al.*, 1993; Voorhees *et al.*, 2010). This gate is rather open in Sso aIF2γ because Ile61 is replaced by Met45 in the equivalent position (the minimal distance

between Val18 and Met45 in Sso aIF2γ is 6.03 Å instead of 4.31 Å between Val19 and Ile61 in Tth EF-Tu; Supplementary Fig. S1*b*). Therefore, in Sso aIF2γ a spontaneous rotation of His97 around its $C^{\alpha}-C^{\beta}$ bond is able to push water molecule A618 towards the γ-phosphate and correctly align it along the PG—O3B axis for nucleophilic attack (Daviter *et al.*, 2003; Voorhees *et al.*, 2010). As a result, GTP hydrolysis can occur and the hydrogen bond between the γ-phosphate and the main-chain amide N atom of Gly96 can be broken.

In the S2 structure, the formate ion possibly mimics P_i (Supplementary Fig. S3). This ion is more hydrophobic than P_i and forms partly inaccessible hydrogen bonds to both switch regions. Based on the S2 and Sso aIF2$\alpha3\beta\gamma$ (Yatime *et al.*, 2007) structures, it is possible to suggest that the inorganic phosphate does not escape from aIF2γ immediately after hydrolysis. However, as was shown in the MD experiments (Satpati & Simonson, 2012), dissociation of P_i from aIF2γ is highly favourable and the protein switches spontaneously and quickly from the ON state to the OFF state. This result is in reasonably good agreement with the high GDP/GTP-exchange rate observed for Sso aIF2 (Pedullà *et al.*, 2005). On the other hand, no significant hydrolysis was observed by this group in their kinetic experiments and they suggest that 'the interaction of the factor with the ribosome, even in the presence of codon–anticodon pairing, is not sufficient by itself to trigger the reaction' (Pedullà *et al.*, 2005).

4.2. Hydrolysis of GTP and GDP/GTP exchange in eukaryotes

The amino-acid sequences of translation initiation factors 2 are conserved in archaea and eukaryotes (Supplementary Fig. S1*a*), suggesting that they share a common three-dimensional structure (Schmitt *et al.*, 2002; Roll-Mecak *et al.*, 2004; Sokabe *et al.*, 2006). The highest sequence conservation occurs within the canonical nucleotide-binding pocket (with an amino-acid sequence identity of about 65%). Nonetheless, eukaryal IF2 has a much higher affinity for GDP (3.0×10^{-8} *M*) than for GTP (2.5×10^{-6} *M*) (Walton & Gill, 1975) and requires the GDP/GTP-exchange factor eIF2B to be reactivated after GTP hydrolysis. In *S. solfataricus*, the γ subunit and intact aIF2 have a similar affinity for GDP and GTP (Pedullà *et al.*, 2005).

In eukaryotes, several amino-acid substitutions in the P loop, helix $\alpha1$ and the switch 1 and switch 2 regions (Supplementary Fig. S1*b*) are able to reduce the GTP-hydrolysis rate. Some of them (Val14Thr and Ala94Cys) stabilize the ON state of switch 2 in eIF2γ through additional hydrogen bonds, while others (His37Phe, Ser38Lys, Gly44Asn and Met45Ile) stabilize the αA helix in the switch 1 region and promote closure of the nucleotide-binding pocket. Therefore, it is possible to suggest that similar to as in EF-Tu (Berchtold *et al.*, 1993; Kjeldgaard *et al.*, 1993) switch 1 plays the role of a cover for the nucleotide-binding pocket, which is predominantly closed in eIF2γ and open in aIF2γ. This explains the presence of eIF5 and eIF2B in eukaryotic cells. Notably, the αA* helix of the switch 1 region (Supplementary Fig. S1) closes the nucleotide-binding pocket in the EF-Tu–GDP structure, while both the αA and αA* helices of this switch are used to close the pocket in the EF-Tu–GTP structure. Possibly, the closed nucleotide-binding pocket is required for eIF2 and EF-Tu to retain P_i over a long period of time and to increase the interval required for tRNA binding.

The coordinates and structure factors for the crystal structures of aIF2γ in different states (S1, S2, S3 and S4) have been deposited in the Protein Data Bank as entries 4m53, 4m4s, 4m0l and 4m2l, respectively.

This research was supported by the Russian Academy of Sciences, the Russian Foundation for Basic Research and the Program of RAS on Molecular and Cellular Biology. We thank A. G. Gabdulkhakov and A. D. Nikulin for the diffraction data collection.

References

Adams, P. D., Grosse-Kunstleve, R. W., Hung, L.-W., Ioerger, T. R., McCoy, A. J., Moriarty, N. W., Read, R. J., Sacchettini, J. C., Sauter, N. K. & Terwilliger, T. C. (2002). *Acta Cryst.* D**58**, 1948–1954.
Algire, M. A., Maag, D. & Lorsch, J. R. (2005). *Mol. Cell*, **20**, 251–262.
Arai, K., Arai, N., Nakamura, S., Oshima, T. & Kaziro, Y. (1978). *Eur. J. Biochem.* **92**, 521–531.
Berchtold, H., Reshetnikova, L., Reiser, C. O., Schirmer, N. K., Sprinzl, M. & Hilgenfeld, R. (1993). *Nature (London)*, **365**, 126–132.
Brünger, A. T., Adams, P. D., Clore, G. M., DeLano, W. L., Gros, P., Grosse-Kunstleve, R. W., Jiang, J.-S., Kuszewski, J., Nilges, M., Pannu, N. S., Read, R. J., Rice, L. M., Simonson, T. & Warren, G. L. (1998). *Acta Cryst.* D**54**, 905–921.
Daviter, T., Wieden, H.-J. & Rodnina, M. V. (2003). *J. Mol. Biol.* **332**, 689–699.
Emsley, P., Lohkamp, B., Scott, W. G. & Cowtan, K. (2010). *Acta Cryst.* D**66**, 486–501.
Kabsch, W. (1993). *J. Appl. Cryst.* **26**, 795–800.
Kjeldgaard, M., Nissen, P., Thirup, S. & Nyborg, J. (1993). *Structure*, **1**, 35–50.
Knudsen, C., Wieden, H.-J. & Rodnina, M. V. (2001). *J. Biol. Chem.* **276**, 22183–22190.
Krab, I. M. & Parmeggiani, A. (1998). *Biochim. Biophys. Acta*, **1443**, 1–22.
Kyrpides, N. C. & Woese, C. R. (1998). *Proc. Natl. Acad. Sci. USA*, **95**, 3726–3730.
Li, G. & Zhang, X. C. (2004). *J. Mol. Biol.* **340**, 921–932.
Liljas, A., Ævarsson, A., al-Karadaghi, S., Garber, M., Zheltonosova, J. & Brazhnikov, E. (1995). *Biochem. Cell Biol.* **73**, 1209–1216.
Nikonov, O., Stolboushkina, E., Nikulin, A., Hasenöhrl, D., Bläsi, U., Manstein, D. J., Fedorov, R., Garber, M. & Nikonov, S. (2007). *J. Mol. Biol.* **373**, 328–336.
Pedullà, N., Palermo, R., Hasenöhrl, D., Bläsi, U., Cammarano, P. & Londei, P. (2005). *Nucleic Acids Res.* **33**, 1804–1812.
Polekhina, G., Thirup, S., Kjeldgaard, M., Nissen, P., Lippmann, C. & Nyborg, J. (1996). *Structure*, **4**, 1141–1151.
Roll-Mecak, A., Alone, P., Cao, C., Dever, T. E. & Burley, S. K. (2004). *J. Biol. Chem.* **279**, 10634–10642.
Satpati, P. & Simonson, T. (2012). *Biochemistry*, **51**, 353–361.
Schmitt, E., Blanquet, S. & Mechulam, Y. (2002). *EMBO J.* **21**, 1821–1832.
Simonetti, A., Marzi, S., Fabbretti, A., Hazemann, I., Jenner, L., Urzhumtsev, A., Gualerzi, C. O. & Klaholz, B. P. (2013). *Acta Cryst.* D**69**, 925–933.
Sokabe, M., Yao, M., Sakai, N., Toya, S. & Tanaka, I. (2006). *Proc. Natl Acad. Sci. USA*, **103**, 13016–13021.
Song, H., Parsons, M. R., Rowsell, S., Leonard, G. & Phillips, S. E. V. (1999). *J. Mol. Biol.* **285**, 1245–1256.

Stolboushkina, E., Nikonov, S., Nikulin, A., Bläsi, U., Manstein, D. J., Fedorov, R., Garber, M. & Nikonov, O. (2008). *J. Mol. Biol.* **382**, 680–691.
Stolboushkina, E., Nikonov, S., Zelinskaya, N., Arkhipova, V., Nikulin, A., Garber, M. & Nikonov, O. (2013). *J. Mol. Biol.* **425**, 989–998.
Storoni, L. C., McCoy, A. J. & Read, R. J. (2004). *Acta Cryst.* D**60**, 432–438.
Vetter, I. R. & Wittinghofer, A. (2001). *Science*, **294**, 1299–1304.
Voorhees, R. M., Schmeing, T. M., Kelley, A. C. & Ramakrishnan, V. (2010). *Science*, **330**, 835–838.
Walton, G. M. & Gill, G. N. (1975). *Biochim. Biophys. Acta*, **390**, 231–245.
Yatime, L., Mechulam, Y., Blanquet, S. & Schmitt, E. (2006). *Structure*, **14**, 119–128.
Yatime, L., Mechulam, Y., Blanquet, S. & Schmitt, E. (2007). *Proc. Natl Acad. Sci. USA*, **104**, 18445–18450.